

Beyond scaling and locality in turbulence

A. Bershadskii

ICAR, P.O. Box 31155, Jerusalem 91000, Israel

An analytic perturbation theory is suggested in order to find finite-size corrections to the scaling power laws. In the frame of this theory it is shown that the first order finite-size correction to the scaling power laws has following form $S(r) \cong cr^{\alpha_0} [\ln(r/\eta)]^{\alpha_1}$, where η is a finite-size scale (in particular for turbulence, it can be the Kolmogorov dissipation scale). Using data of laboratory experiments and numerical simulations it is shown that a degenerate case with $\alpha_0 = 0$ can describe turbulence statistics in the near-dissipation range $r > \eta$, where the ordinary (power-law) scaling does not apply. For moderate Reynolds numbers the degenerate scaling range covers almost the entire range of scales of velocity structure functions (the log-corrections apply to finite Reynolds number). Interplay between local and non-local regimes has been considered as a possible hydrodynamic mechanism providing the basis for the degenerate scaling of structure functions and extended self-similarity. These results have been also expanded on passive scalar mixing in turbulence. Overlapping phenomenon between local and non-local regimes and a relation between position of maximum of the generalized energy input rate and the actual crossover scale between these regimes are briefly discussed.

PACS numbers: 47.27.-i, 47.27.Gs

I. INTRODUCTION

Scaling and related power laws are widely used in physics. In real situations, however, scaling holds only approximately. As a consequence, the corresponding scaling power laws hold approximately as well. On the other hand, discovery of the extended self-similarity in turbulence [1],[2] and in the critical phenomena (see for a review [3],[4]) shows that universal laws similar to the scaling ones can go far beyond the scaling itself, both for velocity [1],[2] and for different fields convected by turbulence [5],[6]. The question is: does the extended self-similarity (ESS) can be theoretically explored in the frames of general scaling ideas or one needs in a completely new frames to explain the ESS? In turbulence this problem is related to the problem of the so-called near-dissipation range. Theoretical approach to description of the scaling (the so-called inertial) range of scales in turbulence requires that the space scales $r \gg \eta$, where η is (Kolmogorov) dissipation or molecular viscous scale [7, 8]. On the other hand, the near-dissipation range of scales, for which $r > \eta$ has a more complex, presumably non-scaling dynamics (see, for instance, Refs.[9]-[15] and the references cited there). Indeed, for moderate Reynolds numbers, the near-dissipation range can span most of the available range of scales [12]. Different perturbation theories, which start from scaling as a leading mode, can be developed. Effectiveness of such theories is usually checked by comparison with experiments. In the present paper we will explore a generic analytic expansion of scaling in direction of the dissipation scale η . Effectiveness of the suggested perturbation theory has been shown for the turbulent flows with moderate Reynolds numbers. Interplay between local and non-local regimes has been considered as a possible hydrodynamic mechanism providing the basis for the degenerate scaling of structure functions and extended self-similarity in turbulent flows.

II. ANALYTIC PERTURBATIONS TO SCALING

Let us consider a dimensional function $S(r)$ of a dimensional argument r . And let us construct a *dimensionless* function of the same argument

$$\alpha(r) = \frac{S^{-1}dS}{r^{-1}dr}. \quad (1)$$

If for $L \gg r \gg \eta$ we have no relevant fixed scale (scaling situation), then for these values of r the function $\alpha(r)$ must be independent on r , i.e. $\alpha(r) \simeq const$ for $L \gg r \gg \eta$. Solution of equation (1) with constant α can be readily found as

$$S(r) \cong cr^\alpha \quad (2)$$

where c is a dimension constant. This is the well-known power law corresponding to the scaling situations.

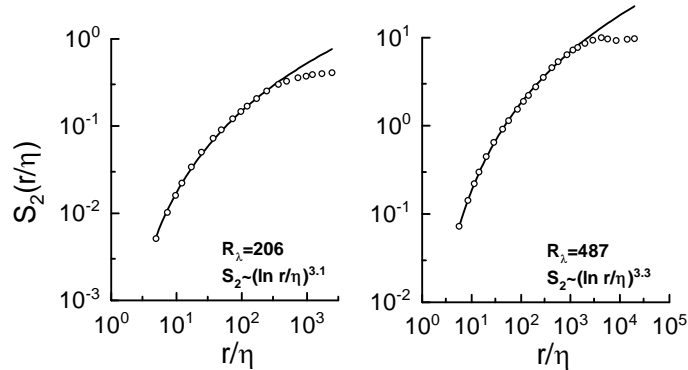


FIG. 1: The second order structure function $S_2(r/\eta)$ against r/η . The experimental data ($R_\lambda = 206, 487$) [17] are shown as circles. The solid curves are the best fit of (7) to the data, corresponding to the degenerated scaling.

Let us now consider an analytic theory, which allows us to find generic corrections of all orders to the approximate power law, related to the fixed small scale η . In the non-scaling situation let us denote

$$f \equiv \ln(S/A), \quad x \equiv \ln(r/\eta) \quad (3)$$

where A and η are dimensional constants used for normalization.

In these variables, equation (1) can be rewritten as

$$\frac{df}{dx} = \alpha(x) \quad (4).$$

In the non-scaling situation x is a dimensionless variable, hence the dimensionless function $\alpha(x)$ can be non-constant. Since the 'pure' scaling corresponds to $x \gg 1$ we will use an analytic expansion in power series

$$\alpha(x) = \alpha_0 + \frac{\alpha_1}{x} + \dots + \frac{\alpha_n}{n!x^n} + \dots \quad (5)$$

where α_n are dimensionless constants. After substitution of the analytic expansion (5) into Eq. (4) the zeroth order approximation gives the power law (2) with $\alpha \cong \alpha_0$. First order analytic approximation, when one takes only the two first terms in the analytic expansion (5), gives

$$S(r) \cong cr^{\alpha_0} [\ln(r/\eta)]^{\alpha_1}. \quad (6)$$

This is a generic analytic first order approximation to the scaling power laws provided by the perturbation theory suggested above.

Corrections of the higher orders can be readily found in this perturbation theory.

For degenerate case with $\alpha_0 = 0$ the second term in the expansion (5) becomes the leading term

$$S(r) \sim [\ln(r/\eta)]^{\alpha_1} \quad (7)$$

It was already mentioned that there are many different ways to develop perturbation theory to scaling. The idea that just $\ln(r/\eta)$ is an appropriate parameter for the finite-size corrections to scaling in turbulence was suggested in [15]. On a physical level this was related in [15] to the instabilities of the thin vortex tubes (or filaments), which are the most prominent hydrodynamical elements of turbulent flows. These instabilities usually appear as kinks readily transforming into wave packets propagating along the filaments. One can consider such wave packet with scale r and make use of the "localized induction" approximation to the Biot-Savart formula [16]. In this approximation, contributions of portions at distances greater than $\sim r \gg \eta$ to the velocity fluctuation in the immediate vicinity of any given point on the filament are neglected. The vortex core radius, which usually associated with η , provides a cutoff from below. The vortex filament dynamics in this approximation is described by the equation

$$\frac{d\mathbf{X}}{dt} = \frac{\Gamma}{4\pi} \left\{ \ln \left(\frac{r}{\eta} \right) \right\} \gamma \mathbf{b}$$

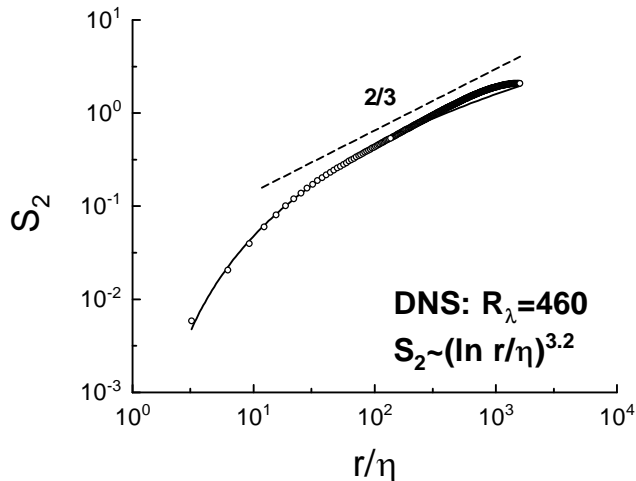


FIG. 2: The second order structure function $S_2(r/\eta)$ against r/η . The DNS data [18] ($R_\lambda = 460$) are shown as circles. The solid curve is the best fit of (7) corresponding to the degenerated scaling.

where \mathbf{X} is the position vector of a point on the filament, Γ is the vortex strength, γ is the local curvature, and \mathbf{b} is the unit binormal vector of the filament. One can see that in this approximation the dependence on r is completely determined by the logarithmic term $\ln(r/\eta)$ in the dynamic equation. This pure hydrodynamic consideration was suggested in [15] as a basis for using just $\ln(r/\eta)$ in finite-size corrections to scaling in turbulence (see also Section IV below).

III. TURBULENCE

The longitudinal structure function of order p for the velocity field [7]

$$S_p(r) = \langle |\Delta u|^p \rangle \quad (8)$$

($\Delta u = (\mathbf{u}(\mathbf{r} + \mathbf{x}) - \mathbf{u}(\mathbf{r})) \cdot \mathbf{r}/r$) calculated for $p = 2$, using the data obtained in a wind tunnel at $R_\lambda = 206$ and 487 [17], is shown in Fig. 1. Here R_λ is the so-called Taylor microscale Reynolds number. The experiment with a flow, which was a combination of the wake and homogeneous turbulence behind a grid, is described in Ref. [17]. We invoke Taylor's hypothesis [7] to equate temporal statistics to spatial statistics.

The solid curves in these figures are the best fit by equation (7) corresponding to the degenerate scaling. Figure 2 shows $S_2(r)$ calculated using data from a high-resolution direct numerical simulation of homogeneous steady three-dimensional turbulence [18], corresponding to 1024^3 grid points and $R_\lambda = 460$. The solid curve in this figure also corresponds to the best fit by equation (7). As far as we know Eq. (7) was suggested as an empirical approximation of the structure functions for the first time in our earlier paper [12]. Application of these results to correlation functions [7] is in good agreement with the structure functions analysis (cf. for instance, Figs. 1 and 3).

Figure 4 shows the structure functions of different orders p for the wind-tunnel data ($R_\lambda = 487$) and the degenerate scaling (7) is shown in the figure as the solid curves. One can see that the degenerate scaling requires two fitting constants just as the ordinary scaling does, and, in the examples discussed above, the range of scales covered by the degenerate scaling is about two decades.

IV. A POSSIBLE HYDRODYNAMIC SCENARIO

In order to understand a possible hydrodynamic mechanism of the phenomenon described above let us recall that in isotropic turbulence a complete separation of local and non-local interactions is possible in principle. It was shown

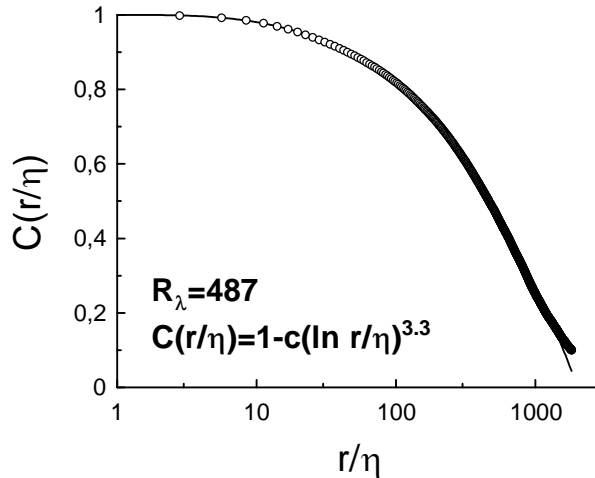


FIG. 3: Correlation function for velocity fluctuations against $\log r/\eta$ for $R_\lambda = 487$ (circles) [17]. The solid curve is drawn in the figure to indicate agreement with the degenerate scaling shown in Fig. 1.

by Kadomtsev [20] that this separation plays a crucial role for the local Kolmogorov's cascade regime with scaling energy spectrum

$$E(k) \sim \bar{\varepsilon}^{2/3} k^{-5/3} \quad (9)$$

where $\bar{\varepsilon}$ is the average of the energy dissipation rate, ε , $k \sim 1/r$ is the wave-number. This separation should be effective for the both ends. That is, if there exists a solution with the local scaling (9) as an asymptote, then there should also exist a solution with the non-local scaling asymptote. Of course, the two solutions with these asymptotes should be alternatively stable (unstable) in different regions of scales. It is expected, that the local (Kolmogorov's) solution is stable (i.e. statistically dominating) in inertial range (that means instability of the non-local solution in this range of scales).

Roughly speaking, in non-local solution for small scales r only non-local interactions with large scales L ($1 \gg r/L$) are dynamically significant and the non-local interactions is determined by large scale strain/shear. This means that one should add to the energy flux $\bar{\varepsilon}$ -parameter (which is a governing parameter for the both solutions) an additional parameter such as the strain s for the non-local solution. As far as we know it was noted for the first time by Nazarenko and Laval [21] that dimensional considerations applied to the non-local asymptotic result in the power-law energy spectrum

$$E(k) \sim \frac{\bar{\varepsilon}}{s} k^{-1} \quad (10)$$

both for two- and three-dimensional cases. Linear dependence of the spectrum (10) on $\bar{\varepsilon}$ is determined by the linear nature of equations corresponding to the non-local asymptotic that together with the dimensional considerations results in (10) [21]. Interesting numerical simulations were performed in [22]. In these simulations local and non-local interactions have been alternatively removed. For the first case a tendency toward a spectrum flatter than '-5/3' is observed near and beyond the separating scale (beyond which local interactions are ignored), that supports Eq. (10) (see also below).

Following to the perturbation theory suggested in Section II both local and non-local regimes can be corrected. The first order correction is

$$E(k) \sim k^{-5/3} [\ln(k_d/k)]^\gamma \quad (11)$$

and

$$E(k) \sim k^{-1} [\ln(k_d/k)]^\beta \quad (12)$$

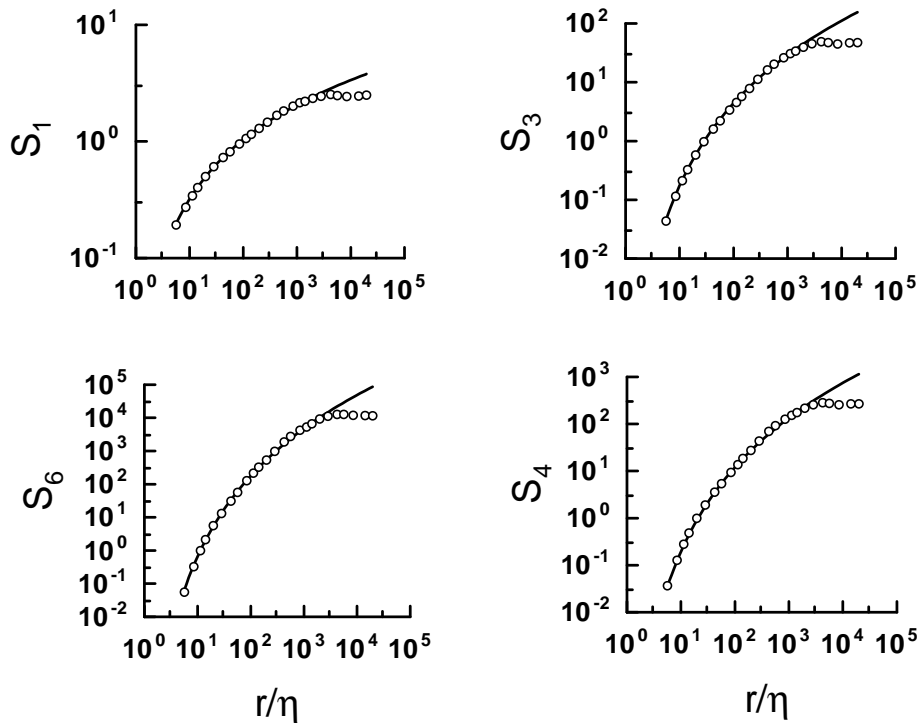


FIG. 4: As in Fig. 1 ($R_\lambda = 487$) but for different orders of the structure function.

(where $k_d \equiv 1/\eta$) for the local and non-local regimes respectively (γ and β are dimensionless constants). In the case when $\beta \gg \gamma$ the first order finite-size correction in the non-local regime becomes substantial much 'earlier' (i.e. for smaller k) than for the local (Kolmogorov's) regime (see Eq. (5)). This can result in viscous stabilization of the non-local regime (cf [22]) and, as a consequence, in the so-called 'exchange of stability' phenomenon at certain $k_c = 1/r_c$. That is, for $k < k_c$ the Kolmogorov's regime is stable and the non-local regime is unstable, whereas for $k > k_c$ the Kolmogorov's regime is unstable and the non-local regime is stable. For this scenario, at $k = k_c$ the Kolmogorov's regime is still asymptotically scale-invariant (i.e. Eq. (9) gives an adequate approximation for this regime), while for the non-local regime the first order correction is substantial (i.e. Eq. (12) should be used at $k = k_c$ for the non-local regime). In this scenario the Kolmogorov's regime plays significant role in the viscous stabilization of the non-local regime for $k > k_c$ (cf [22]), but for these k the non-local regime becomes statistically dominating instead of the Kolmogorov's one. Figure 5 shows a spectrum measured in nearly isotropic turbulence downstream of an active grid at $R_\lambda = 716$ (the data are reported in [19]). The solid curve is drawn in the figure to indicate correspondence of the data to the equation (12) (non-local regime), while the dashed straight line indicates the Kolmogorov's "-5/3" law to show possible interplay between the Kolmogorov's and non-local regimes at this Reynolds number.

If one tries to estimate the second order structure function $S_2(r)$ as [7]

$$S_2(r) \sim \int_{1/r}^{1/\eta} E(k) dk \quad (13)$$

for $r < r_c$ using Eq. (12), one obtains

$$S_2(r) \sim [\ln(r/\eta)]^{\zeta_2} \quad (14)$$

with $\zeta_2 = \beta + 1$ (cf Section 3). For instance, for the data shown in Fig. 5 we obtain $\zeta_2 \simeq 3.9$. Comparing figures 1,2 and 5 one can see that α is monotonically increased with Re_λ .

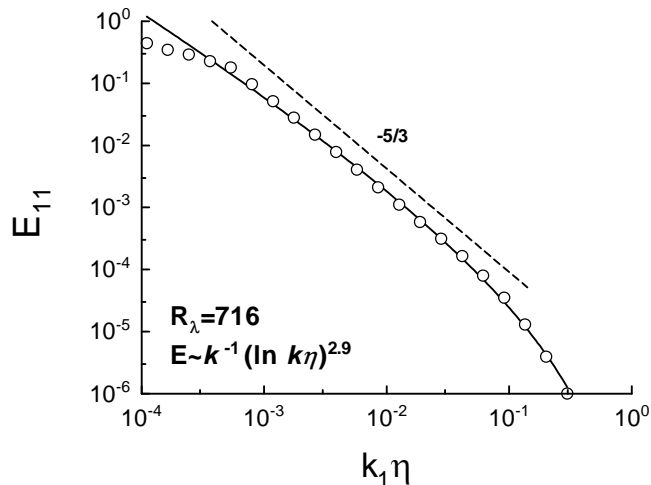


FIG. 5: Longitudinal energy spectrum against $k\eta$ in log-log scales. The data (circles) correspond to a nearly isotropic (active-) grid turbulence $R_\lambda = 716$ [19]. The solid curve is drawn in the figure to indicate agreement with the Eq. (12), while the dashed straight line indicates the “-5/3” Kolmogorov’s law.

Let us generalize (13) introducing an effective spectrum $E_n(k)$

$$S_n(r) \sim \int_{1/r}^{1/\eta} E_n(k) dk \quad (15)$$

($E_2(k) \equiv E(k)$). Then using the dimensional considerations we obtain for the non-local regime

$$E_n(k) \sim \left(\frac{\bar{\epsilon}}{s}\right)^{n/2} k^{-1} \quad (16)$$

The first order correction is

$$E_n(k) \sim \left(\frac{\bar{\epsilon}}{s}\right)^{n/2} k^{-1} [\ln(k_d/k)]^{\beta_n} \quad (17)$$

Substituting (17) into (15) one obtains

$$S_n(r) \sim \left(\frac{\bar{\epsilon}}{s}\right)^{n/2} [\ln(r/\eta)]^{\zeta_n} \quad (18)$$

with $\zeta_n = \beta_n + 1$.

Thus the non-local regime can provide hydrodynamic basis for the degenerate scaling of the structure functions.

V. EXTENDED SELF-SIMILARITY

In our previous paper [12] we discussed possible relation between ESS and structure functions given by Eq. (7). Now we can elaborate this relation with more details. While in the near-dissipation range we observe the degenerate scaling an ordinary scaling (presumably Kolmogorov’s one) has been certainly observed in the inertial range of scales for very large Reynolds numbers (see, for instance, [7],[23]). Therefore, one can expect the existence of a crossover scale r_c from the ordinary scaling to the degenerate one (see previous section). At the scale $r = r_c$ we can use a continuity condition between ordinary scaling (2) and degenerate scaling (7)

$$cr_c^{\zeta'_2} = A[\ln(r_c/\eta)]^{\zeta_2} \quad (19)$$

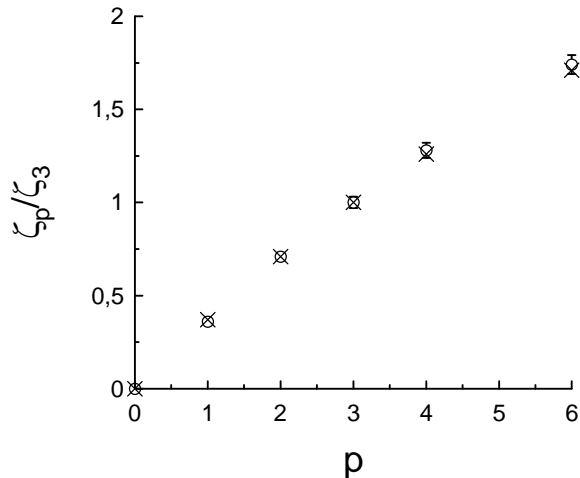


FIG. 6: Normalized exponents ζ_p/ζ_3 against p for $R_\lambda = 487$ (circles). The exponents were obtained using the data shown in Figs. 1,4. Crosses are the ESS exponents obtained for the atmospheric turbulence data at $R_\lambda = 10340$ [23].

for the structure functions of all orders (c and A are some constants). Let us denote in general case

$$S_p(r) = A'_p r^{\zeta'_p}; \quad S_p(r) = A_p [\ln(r/\eta)]^{\zeta_p} \quad (20)$$

in inertial and near-dissipation ranges respectively.

Then condition of compatibility of the continuity equations (19) for different order (m and n) structure functions

$$A'_m r_c^{\zeta'_m} = A_m [\ln(r_c/\eta)]^{\zeta_m}; \quad A'_n r_c^{\zeta'_n} = A_n [\ln(r_c/\eta)]^{\zeta_n} \quad (21)$$

can be of two kinds.

The first kind is applicable for arbitrary value of r_c and has the form

$$\frac{\zeta_m}{\zeta_n} = \frac{\zeta'_m}{\zeta'_n}; \quad \left(\frac{A'_m}{A_m}\right)^{\zeta_n} = \left(\frac{A'_n}{A_n}\right)^{\zeta_m} \quad (22)$$

while another kind is applicable for a fixed value of r_c only. Below we will be interested in the first kind of the compatibility condition. This condition, in particular, gives a power-law relation between moments of different orders

$$S_m(r) \sim S_n^{\beta_{m,n}}(r), \quad (23)$$

with the same exponent

$$\beta_{m,n} = \frac{\zeta'_m}{\zeta'_n} = \frac{\zeta_m}{\zeta_n} \quad (24)$$

for both inertial and near-dissipation ranges (see Eq. (22)). The last phenomenon was previously observed in different turbulent flows and was called Extended Self-Similarity (ESS) [1],[2],[12]. It is important to note that at ESS not only the scalings (23) are the same in both regimes inertial and dissipative, but also the prefactors are the same. Figure 6 shows as circles the exponents ζ_p obtained from Figs. 1,4 and normalized by the exponent ζ_3 . For comparison we show by crosses in this figure the normalized exponents obtained using ESS in the atmospheric turbulence for large $R_\lambda = 10340$ [23].

It should be noted that a high-resolution numerical simulation reported in a recent paper [13] for *low-Reynolds-number* ($R_\lambda \approx 10-60$) flows shows no hint of scaling-like behavior of the velocity increments even when ESS is applied.

That should return us to the Section II and recall us that the degenerate scaling in the form of Eq. (7) is only a *first* non-trivial term in the perturbation theory. Moreover, the question of convergence of the perturbation theory used in Section II become significant at the *low-Reynolds-number*, when the dissipation scale is effectively too close to the scales under consideration. Though, the authors of Ref. [13] claim that: 'the DNS scaling exponents of velocity gradients agree well with those deduced, using a recent theory of anomalous scaling, from the scaling exponents of the longitudinal structure functions at infinitely high Reynolds numbers. This suggests that the asymptotic state of turbulence is attained for the velocity gradients at far lower Reynolds numbers than those required for the inertial range to appear'. This circle of problems can be also related to the possibility of fluctuations of the dissipation scale [13],[14]. For the cases when these fluctuations are significant a set of the expansions might be needed or (alternatively, for moderate Reynolds numbers) calculation should involve averaging over the fluctuating cut-off η . In the last case the experimental and numerical data suggest that the average value of η should not deviate strongly from the Kolmogorov dissipation scale (at least for the moderate values of Reynolds number).

Though, the problem with the small Reynolds numbers can be deeper. We do not know whether the non-local regime appears at the same Reynolds number as the local one. The energy balance of the non-local regime is more complex than that of the local one. Actually the non-local regime needs in the local one (even statistically unstable) for this balance (cf [22]). Therefore, *critical* Reynolds number for appearance of the (stable) non-local regime can be larger than that for the local regime.

VI. GENERALIZED ENERGY INPUT RATE

Figures 2 and 5 show that for sufficiently large Reynolds numbers, providing a visible inertial interval, there is an overlapping between the two scalings: non-local and local (Kolmogorov). This overlapping is based on the very nature of the stability exchange between the two *statistical* regimes. Therefore, it is not a simple task to determine the scale r_c from the $S_n(r)$ -data. A more fine information one can infer studying

$$D_{LLL}(r) = \langle \Delta u^3 \rangle$$

(cf Eq.(8) and see [7],[15],[18]). Unlike S_3 most positive contributions are canceled by negative ones in D_{LLL} , and only the slight asymmetry of the Δu probability density contributes to D_{LLL} . However, this asymmetry has a fundamental nature. Therefore, one can expect that the above used dimensional considerations can be also used for D_{LLL} for the both non-local and local regimes. For the local (Kolmogorov) regime one has [7],[15],[18]

$$-D_{LLL} \sim \bar{\varepsilon} r \quad (25)$$

while for the degenerate scaling

$$-D_{LLL} \sim \left(\frac{\bar{\varepsilon}}{s}\right)^{3/2} [\ln(r/\eta)]^\delta \quad (26)$$

Figure 7 shows $-D_{LLL}$ (as circles) and $-D_{LLL}/\bar{\varepsilon}r$ (as crosses) calculated using data from the direct numerical simulation of homogeneous steady three-dimensional turbulence [18]. The solid curve in this figure corresponds to the best fit by equation (26). In this figure one can see that the overlapping between the two regimes exists even for the D_{LLL} (cf Fig. 2). However, a generalized energy input rate related to D_{LLL} [15] could give a key to our problem. Let us consider the Navier-Stokes equations for a viscous incompressible fluid, given by

$$\frac{\partial u_i}{\partial t} + u_j \frac{\partial u_i}{\partial x_j} = -\frac{1}{\rho} \frac{\partial p}{\partial x_i} + \nu \frac{\partial^2 u_i}{\partial x_j^2} + f_i(\mathbf{x}, t), \quad (27a)$$

$$\frac{\partial u_i}{\partial x_i} = 0, \quad (27b)$$

where $\mathbf{f}(\mathbf{x}, t)$ is random force, ν is kinematic viscosity and ρ is the fluid density. \mathbf{f} will be assumed to be Gaussian with zero mean and a rapidly oscillating character, or a δ -correlation in time. The second-rank correlation tensor

$$\langle f_i(\mathbf{x} + \mathbf{r}, t + \tau) f_j(\mathbf{x}, t) \rangle \sim F_{ij}(\mathbf{r}) \delta(\tau). \quad (28)$$

defines such fields. It was shown in [24] using Eqs. (27) and (28) that S_2 and D_{LLL} are related by the equation

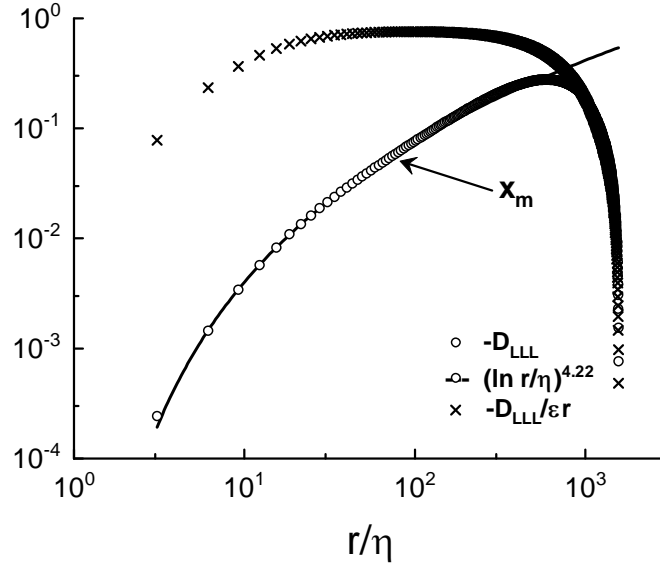


FIG. 7: The DNS data [18] ($R_\lambda = 460$) are shown against r/η as the symbols: $-D_{LLL}$ -circles and $-D_{LLL}/\bar{\epsilon}r$ -crosses. The solid curve is the best fit of (26) corresponding to the degenerated scaling.

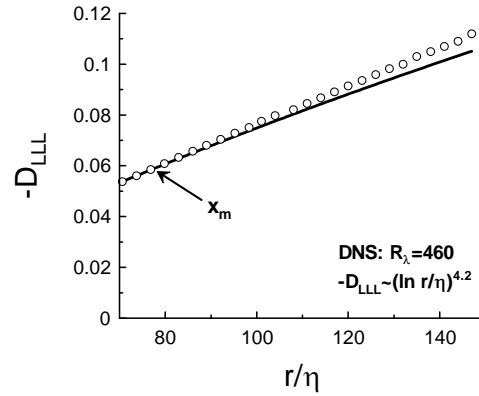


FIG. 8: $-D_{LLL}$ against r/η . The same data as in Fig. 7 but with higher resolution in a small vicinity of the x_m scale. The solid curve is the best fit of (26) corresponding to the degenerate scaling.

$$D_{LLL} = 6\nu \frac{dS_2}{dr} - \frac{2}{r^4} \int_0^r x^4 F_{ii}(x) dx, \quad (29)$$

It was also shown in [24] that

$$F_{ii}(0) = 2\langle \bar{\epsilon} \rangle. \quad (30)$$

F_{ii} corresponds to an external energy input rate [24] (cf Novikov's relation [24]: $\langle f_i(\mathbf{x}, t) v_j(\mathbf{x}', t) \rangle = \frac{1}{2} F_{ij}(\mathbf{x} - \mathbf{x}')$).

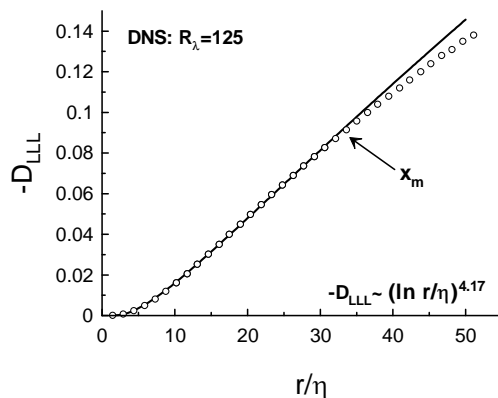


FIG. 9: The same as in Fig. 8 but for $R_\lambda = 125$.

For $r \ll L$ [24]

$$D_{LLL} \simeq 6\nu \frac{dS_2}{dr} - \frac{4}{5} \langle \bar{\varepsilon} \rangle r. \quad (31)$$

When the viscous term can be neglected this gives the Kolmogorov's law (25).

One can formally rewrite (29) as

$$D_{LLL} = -\frac{2}{r^4} \int_0^r x^4 \tilde{F}(x) dx, \quad (32)$$

where the generalized energy input rate is defined as [15]

$$\tilde{F}(x) \equiv F_{ii}(x) - \frac{3\nu d(x^4 dS_2/dx)}{x^4}. \quad (33)$$

Without the second (viscous) term in the right-hand side of Eq. (33) one obtains the Kolmogorov law (25). Therefore, one can associate the first term in the right-hand side of the Eq. (33) with the local (Kolmogorov) regime while the second term can be associated with the non-local one. Gradients of these terms can be associated with local and non-local interaction strengths respectively. Then balance of the local and non-local interaction strengths should be reached at the point given by the equation $d\tilde{F}(x)/dx = 0$. Let us denote position of the balance point as $x = x_m$. One can expect that the crossover scale r_c between the local and non-local regimes (see Section IV) coincides with the balance point of the local and non-local interaction strengths x_m , i.e. $r_c = x_m$. It was shown in [15] that position of the generalized energy input rate maximum $x_m \cong r_m/1.22$, where r_m is position of $-D_{LLL}(r)$ maximum. Since r_m can be obtained from the data this gives us a possibility to estimate r_c from the data as well. For instance, we know [15] that $r_m/\eta \sim R_\lambda^{0.7}$, hence $r_c/\eta \sim R_\lambda^{0.7}$. In Fig. 7 we indicated position of the scale x_m by an arrow and one can see that overlapping of the two regimes can be substantial even for D_{LLL} . In figure 8 we show the same data as in Fig. 7 but with a considerably higher resolution in a small vicinity of the x_m scale. The degenerate scaling fit (solid curve) indeed seems to begin its declination from the data in a small vicinity of the x_m -scale in this case. To support this point we show in figure 9 analogous situation observed for considerably smaller Reynolds number $Re_\lambda = 125$ (see also next Section).

VII. PASSIVE SCALAR

The inertial-convective regime of a passive scalar field transport in isotropic turbulence for large Reynolds numbers is usually described using Obukhov-Corrsin theory [7]. This theory predicts scaling spectrum for the passive scalar (θ) fluctuations with the scaling exponent equal to $-5/3$

$$E^\theta(k) \sim \bar{\varepsilon}^{-1/3} \bar{\varepsilon}_\theta k^{-5/3} \quad (34)$$

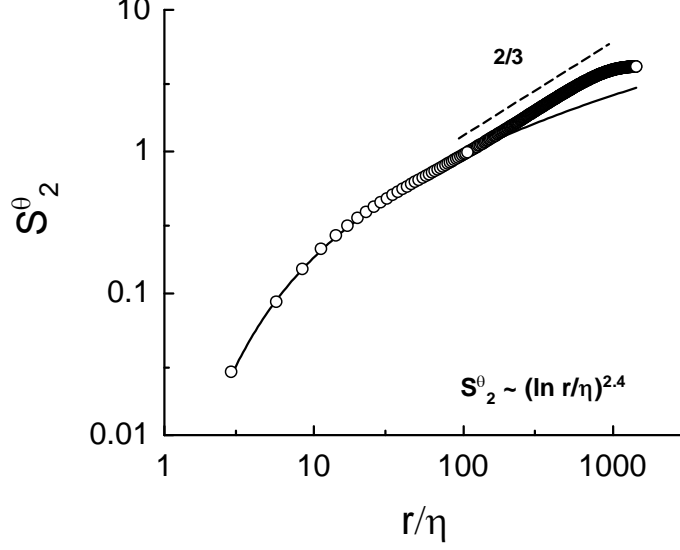


FIG. 10: S_2^θ against r/η . The DNS data (circles) of homogeneous isotropic turbulence described in [28], Péclet number $P_\lambda = 427$ and the Schmidt number is unity (i.e $P_\lambda = R_\lambda$). The solid curve is the best fit to the degenerate scaling (40) (the dashed straight line indicates the Obukhov-Corrsin ordinary scaling [7],[28]).

where $\bar{\varepsilon}_\theta$ is the average value of dissipation rate of scalar variance, ε_θ (cf Eq. (9)). In the experiments, however, this regime is not usually observed (especially, for moderate Reynolds numbers and in turbulent shear flows). In the last case the experiments indicate a strong dependence of the passive scalar spectra on the Reynolds number (see, for instance, Refs. [25], [26] and references therein). In the vein of the Section IV the dimensional considerations applied to the non-local asymptotic result in the power-law spectrum

$$E^\theta(k) \sim \frac{\bar{\varepsilon}_\theta}{s} k^{-1} \quad (35)$$

(cf Eq. (10) and [21],[22],[27]). Accordingly, both scaling regimes (34) and (35) can be corrected (for simplicity we restrict ourselves by the case when the Schmidt number is unity [28]). The first order correction is

$$E_\theta(k) \sim k^{-5/3} [\ln(k_d/k)]^\gamma \quad (36)$$

and

$$E^\theta(k) \sim k^{-1} [\ln(k_d/k)]^\beta \quad (37)$$

for the local and non-local regimes respectively (γ and β are dimensionless constants, different from those in Eqs. (11),(12)).

One can estimate the second order structure function for the passive scalar fluctuations

$$S_2^\theta(r) = \langle |\Delta\theta|^2 \rangle = \langle |\theta(\mathbf{r} + \mathbf{x}) - \theta(\mathbf{r})|^2 \rangle \quad (38)$$

as

$$S_2^\theta(r) \sim \int_{1/r}^{1/\eta} E^\theta(k) dk \quad (39)$$

(cf Eq. (13)). Then for $r < r_c$ using Eqs. (37) and (39) one obtains

$$S_2^\theta(r) \sim [\ln(r/\eta)]^{\zeta_2} \quad (40)$$

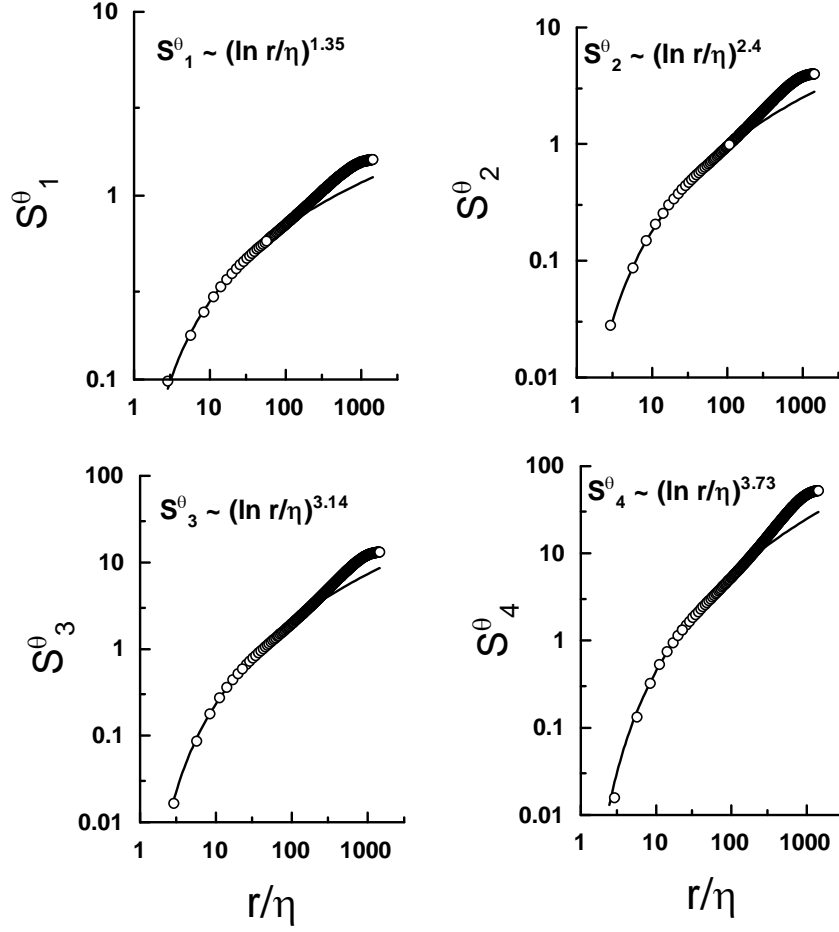


FIG. 11: S_n^θ against r/η . The DNS data (circles) of homogeneous isotropic turbulence described in [28], Péclet number $P_\lambda = 427$ and the Schmidt number is unity (i.e. $P_\lambda = R_\lambda$). The solid curves are the best fit to the degenerate scaling (44).

with $\zeta_2 = \beta + 1$ (cf Section IV).

Figure 10 shows S_2^θ against r/η for the DNS data of homogeneous isotropic turbulence described in [28], Péclet number $P_\lambda = 427$ and the Schmidt number is unity (i.e. $P_\lambda = R_\lambda$). The solid curve is the best fit to the degenerate scaling (40) (the dashed straight line indicates the Obukhov-Corrsin ordinary scaling [7],[28]). As in Section IV we can generalize (39) introducing an effective spectrum $E_n^\theta(k)$

$$S_n^\theta(r) = \langle |\Delta\theta|^n \rangle \sim \int_{1/r}^{1/\eta} E_n^\theta(k) dk \quad (41)$$

($E_2^\theta(k) \equiv E^\theta(k)$). Then using the dimensional considerations we obtain for the non-local regime

$$E_n^\theta(k) \sim \left(\frac{\bar{\varepsilon}_\theta}{s}\right)^{n/2} k^{-1} \quad (42)$$

The first order correction is

$$E_n^\theta(k) \sim \left(\frac{\bar{\varepsilon}_\theta}{s}\right)^{n/2} k^{-1} [\ln(k_d/k)]^{\beta_n} \quad (43)$$

Substituting (43) into (41) one obtains

$$S_n^\theta(r) \sim \left(\frac{\bar{\varepsilon}_\theta}{s}\right)^{n/2} [\ln(r/\eta)]^{\zeta_n} \quad (44)$$

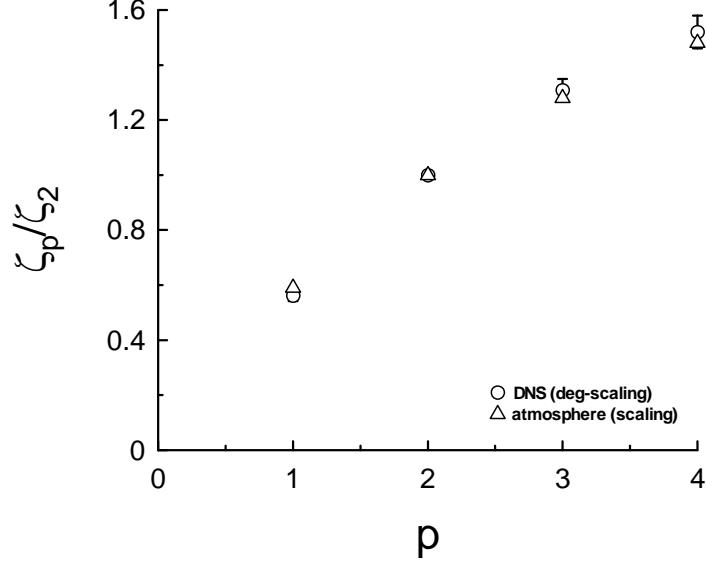


FIG. 12: Exponents extracted from Fig. 11 (circles) and for the fully developed atmospheric turbulence (ordinary scaling in the inertial interval, triangles [29]).

with $\zeta_n = \beta_n + 1$.

Figure 11 shows S_n^θ against r/η for the DNS data of homogeneous isotropic turbulence described in [28], Péclet number $P_\lambda = 427$ and the Schmidt number is unity (i.e $P_\lambda = R_\lambda$). The solid curves are the best fit to the degenerate scaling (44).

One can readily expand the conclusions of the section V regarding Extended Self-Similarity on the case of passive scalar and we show effectiveness of this in figure 12. The data for degenerate scaling (circles) were taken from the degenerate scaling shown in Fig. 11 whereas the data for the ordinary scaling (triangles) were taken from a high Reynolds number atmospheric experiment [29].

The overlapping phenomenon (Section VI) takes also place for the S_n^θ as for S_n . In $\langle \Delta\theta^3 \rangle$ like in D_{LLL} most positive contributions are canceled by negative ones and only the slight asymmetry of the $\Delta\theta$ probability density contributes to $\langle \Delta\theta^3 \rangle$. However, similarly to D_{LLL} this asymmetry has a fundamental nature. Therefore, one can expect that $\langle \Delta\theta^3 \rangle$ also can be used in order to determine r_c . Moreover, since $\langle \Delta\theta^3 \rangle$ as function of r/η has a turnover point, as one can see in figure 13, the turnover point should indicate the point where the actual declination of the degenerate scaling fit from the data should begin. In the turnover point derivative of the function $\langle \Delta\theta^3 \rangle$ has its minimum. In the inset to Fig. 13 we show with high resolution the derivative in a vicinity of its minimum. We also indicate with arrow the position of local maximum of the generalized energy input rate $x_m \simeq r_c$ calculated using D_{LLL} for this case (cf Section VI).

One can see that the suggested perturbation theory with the degenerate scaling is an appropriate tool for description of data in the near-dissipation range. For modest Reynolds numbers the degenerate scaling applies to nearly the entire range of scales. Crossover between the degenerate and ordinary scaling provides an explanation to the Extended Self-Similarity. Interplay between local and non-local interactions can be considered as a possible hydrodynamics mechanisms of these phenomena.

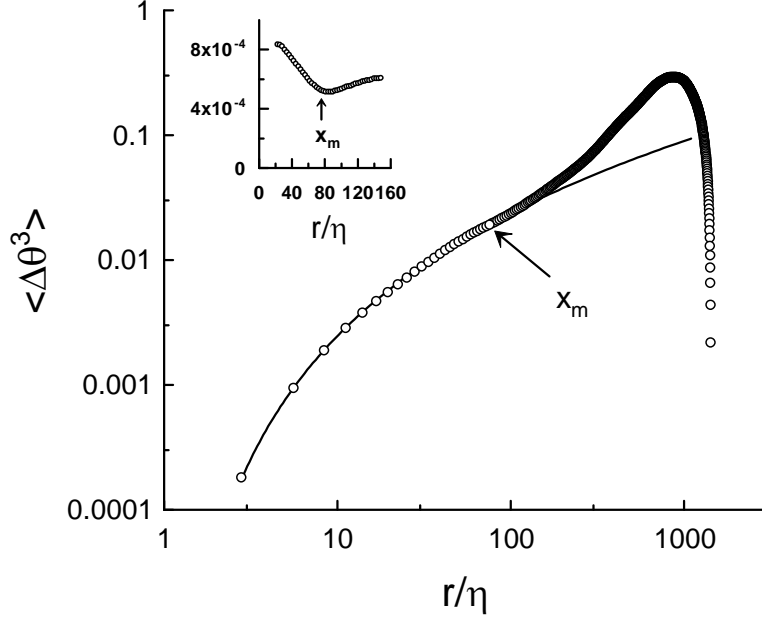


FIG. 13: $\langle \Delta\theta^3 \rangle$ against r/η . The DNS data (circles) of homogeneous isotropic turbulence described in [28], Péclet number $P_\lambda = 427$ and the Schmidt number is unity (i.e $P_\lambda = R_\lambda$). The solid curve is the best fit to the degenerate scaling. The inset shows with high resolution the derivative of $\langle \Delta\theta^3 \rangle$ in a vicinity of its minimum. The arrow indicates position of the generalized energy input rate maximum $x_m \simeq r_c$ calculated using D_{LLL} .

Acknowledgments

I thank K.R. Sreenivasan for inspiring cooperation. Discussions with T. Nakano and V. Steinberg were very useful.

-
- [1] R. Benzi, S. Ciliberto, R. Tripicciono, C. Baudet, F. Massaiolo, and S. Succi, Phys. Rev. E., **48**: R29 (1993).
 - [2] R. Benzi, L. Biferale, S. Ciliberto, M.V. Struglia and R. Tripicciono, Physica D **96**: 162 (1996).
 - [3] D. Sornette, Critical Phenomena in Natural Sciences (Springer, New York 2004).
 - [4] L. Moriconi, A.L.C. Pereira, and P.A. Schulz, Phys. Rev. B **69**: 45109 (2004).
 - [5] K.G. Aivalis, K.R. Sreenivasan, Y. Tsuji, J.C. Kiewicki and C.A. Biloft, Phys. Fluids, **14**: 2439 (2002).
 - [6] A. Bershadskii and K.R. Sreenivasan, Phys. Rev. Lett., **93**: 064501 (2004).
 - [7] A.S. Monin and A.M. Yaglom, Statistical Fluid Mechanics, Vol. 2, (MIT Press, Cambridge 1975)
 - [8] K.R. Sreenivasan and R.A. Antonia, Annu. Rev. Fluid Mech. **29**: 435 (1997)
 - [9] M. Nelkin, Adv. Phys. **43**: 143 (1994).
 - [10] C. Meneveau, Phys. Rev. E **54**: 3657 (1996).
 - [11] T. Nakano, D. Fukayama, A. Bershadskii, and T. Gotoh, J. Phys. Soc. Japan, **71**: 2148 (2002).
 - [12] K.R. Sreenivasan and A. Bershadskii, Pramana, **64**: 315 (2005).
 - [13] J. Schumacher, K. R. Sreenivasan, and V. Yakhot, arXiv:nlin.CD/0604072
 - [14] V. Yakhot, Physica D, **215** 166 (2006).
 - [15] K.R. Sreenivasan and A. Bershadskii, J. Fluid. Mech. **554**: 477 (2006).
 - [16] G.K. Batchelor, G.K. An Introduction to Fluid Dynamics (Cambridge University Press, Cambridge, 1970).
 - [17] B.R. Pearson, P.-A. Krogstad and W. van de Water, Phys. Fluids **14**: 1288 (2002)
 - [18] T. Gotoh, D. Fukayama and T. Nakano, Phys. Fluids, **14**: 1065 (2002)
 - [19] H.S. Kang, S. Chester and C. Meneveau, J. Fluid. Mech., **480**: 129 (2003).

- [20] B.B. Kadomtsev, Plasma Turbulence (Academic Press, New York, 1965).
- [21] S. Nazarenko and J.-P. Laval, J. Fluid Mech., **408**: 301 (2000).
- [22] J.-P. Laval, B. Dubrulle and S. Nazarenko, Phys. Fluids, **13**: 1995 (2001).
- [23] K.R. Sreenivasan and B. Dhruva, Prog. Theor. Phys. Suppl. **130**: 103 (1998)
- [24] E.A. Novikov, Sov. Phys. JETP, **20**: 1290 (1965).
- [25] K.R. Sreenivasan, Phys. Fluids, **8**: 189 (1996).
- [26] Z. Warhaft, Ann. Rev. Fluid Mach., **32**: 203 (2000).
- [27] E. Villiermaux, C. Innocenti and J. Duplat, Phys. Fluids, **13**, 284 (2001).
- [28] T. Watanabe and T. Gotoh, New J. Phys. **6**: Art. No. 40. (2004)
- [29] F. Schmidt, D. Schertzer, S. Lovejoy and Y. Brunet, Europhys. Lett. **34**: 195 (1996).